International Journal of Scientific Research in Modern Science and Technology
ISSN: 2583 -7605 (Online)
© IJSRMST | Vol. 3 | Issue 1 | January 2024
Available online at: https://ijsrmst.com/
DOI: https://doi.org/10.59828/ijsrmst.v3i1.177

Simulation study of Perovskite/Si Monolithic Multijunction Solar Cell

Prem Pratap Singh* and Kripa Shanker Singh

Department of Physics, RBS College, Dr. Bhimrao Ambedkar University, Agra-282002 UP India

***Corresponding Author:** mr.prem@live.com

ABSTRACT

The utilization of perovskite and crystalline-silicon (c-Si) light absorbers in multijunction solar cells presents an exciting opportunity to surpass the efficiency limit of the industry's leading single-junction c-Si solar cells. In this work, we used the Solar Cell Capacitance Simulator (SCAPS-1D) to simulate a monolithic tandem junction solar cell. The solar cell consists of two types of materials: low bandgap and high bandgap. These are layers of perovskites and Si, divided by a window layer of zinc oxide (ZnO), a buffer layer of cadmium sulfide (CdS), a recombination layer of Spiro-MeOTAD/silicon, and a heavily doped back surface field layer formed from n^{++}Si to prevent recombination at the back surface. The impact of di fferent series and shunt resistances, as well as perovskite layer thickness and bandgap, on solar cells' photovoltaic performance has been investigated.

Keywords: Multijunction, Perovskite, Silicon, Solar Cell, SCAPS-1D

1. Introduction

Methylammonium lead triiodide ($CH_3NH_3PbI_3$) is a viable contender for the wide-bandgap absorber, especially with the current surge in organic-inorganic lead halide perovskite photovoltaics. $CH_3NH_3PbI_3$, which has a 1.55 eV bandgap, has developed into an effective absorber of light because of its low inherent voltage loss, sharp absorption edge, charge carrier diffusion lengths longer than 1 μm,[1] and inexpensive processing costs. Tandem solar cells, which use perovskite material that can be produced at a lower temperature and has an tuneable bandgap of 1.48 to 2.23 eV [3], are a viable approach to attain high efficiency at a cheap cost. Presently, multi-junction solar cells offer a promising

approach to achieve ultrahigh efficiencies by integrating absorber materials with different band-gap energies into a single photovoltaic device [4, 5, 6, 7]. For tandem solar cells, PSCs combined with Silicon [8] & Copper Indium Gallium Selenide (CIGS) [9] are hence more suitable. The top sub-cell in the tandem device architecture catches high energy photons and efficiently transforms them into high open-circuit voltage with little loss because of its wide bandgap. Owing to its narrow bandgap, the sub cell at the bottom absorbs the remaining photons having low energy. For the bottom sub cell, usually, Silicon is preferred as it gives the best photovoltaic performance as a whole along with excellent absorption of light for near-infrared photons. According to research, the perovskite/silicon monolithic approach for tandem configuration has shown a maximum efficiency of about 30%, theoretically [10].

The sub-cell for the top in a tandem cell made up of hydrogenated amorphous silicon oxides (a-SiO_z:H) was presented by Si et al., and a power conversion efficiency of 11.4% was reported using a cell structure as a-SiO_z:H/a-Si:H/μc-Si:H/μc-Si:H [11]. The thin film solar cell quadruple junction of the form a-Si:H/a-Si:H/μc-Si:H/μc-Si:H was then developed by Urbain et al. with an efficiency of 13.2%. This thin film solar cell showed high open voltage (V_{oc}) due to which it was employed in an integrated photoelectrochemical water splitting system [12]. Liu et al. obtained a high open circuit voltage (V_{oc}), more than 3 eV and a power conversion efficiency of 15.03% using a configuration as follows: a-SiC_z:H/a-Si:H/a-$Si_{1-x}Ge_x$:H/μc-Si:H [13]. A monolithic structure with tandem design for a solar cell composed of pervoskite/c-Si was proposed by S. Albrecht et al. For the window layer, they utilized MoO_3, and for the buffer layer, they used Spiro-MeOTAD. They were able to achieve an efficiency of 16.8% [14]. F. Sahli et al. [15] put up a fresh concept in solar cells with tandem structure made up of perovskite/Silicon-heterojunction (SHJ). They found 22.7% efficiency using nanocrystalline silicon (nc-Si:H) for the recombination layer. S. Essig et al. built a four terminal multijunction device with an overall efficiency of 32.8% utilizing an n-Si wafer for the bottom sub-cell and two distinct materials (GaAs and InGaP) for the top sub-cell [16]. A novel design for a monolithic tandem junction solar cell was put out by J. Zheng et al. It employs perovskite ($Cs_{0.17}FA_{0.6}Pb(Br_{0.17}I_{0.7})_3$) for the top sub-cell and homo-junction silicon for the bottom sub-cell. After controlling for a number of variables, they attain 21.8% efficiency [17]. A new tandem solar cell structure showing an efficiency of 30.2% was published by H. Ferhati et al. using CZTSSe for the bottom sub-cell and a Se/Ti/Se for the top sub-cell [18]. Recent work by K. Eike et al. tuned the IZO front

electrode and the perovskite absorber in various layers of the perovskite/silicon tandem to get a decreased PCE of 26.0% and J_{sc} noticeably greater than 19 mA/cm^2 [19].

In the current study, we analyzed a monolithic multijunction series-connected solar cell having two perovskite/silicon layer terminals using the SCAPS-1D program. We have examined the effects of bandgap and layer thickness of the perovskite on the PV performance of multijunction solar cells. The influence of series resistance and the shunt resistance on the efficiency of solar cells was also analyzed.

2. Simulation Methodology

Figure 1 illustrates the arrangement of the tandem solar cell being analyzed, comprising seven distinct layers: (i) the window layer, (ii) buffer layer, (iii) light absorber layer with broad bandgap, (iv) tunnel junction, (v) light absorbing layer having narrow bandgap, (vi) layer for back surface field, and (vii) metal contacts. The window layer serves to shield the upper cell surface while facilitating the transfer of photons coming from the sunlight into the light absorbing layer to enhance power generation. Zinc oxide (ZnO) is chosen for its excellent transport properties, including a broad bandgap and a high conductivity of n-type [20]. A buffer layer is strategically placed to minimize the absorption losses and direct minority charge carriers to their particular contacts. Its wide bandgap ensures more photons reach the absorber layer and reduces interface recombination, a common issue in heterojunctions. Cadmium sulfide (CdS) is commonly applied for buffer layers due to its optical transparency, broad bandgap, strong electrical properties, low resistivity and high coefficient of absorption [21]. The absorber layer having wide bandgap, typically composed of perovskite material, acts as the top sub-cell, offering high efficiency, affordability, versatility, and partial translucency [22]. The tunnel junction, forming the fourth layer, mitigates optical and electrical losses between the two absorber layers, preventing the formation of a reverse-biased pn junction and thus, halting current flow. Silicon constitutes the bottom absorber layer, with a strongly doped p-type silicon back surface field employed to minimize carrier recombination losses. Table 1 provides a comprehensive overview of the parameters for each material utilized in the configuration.

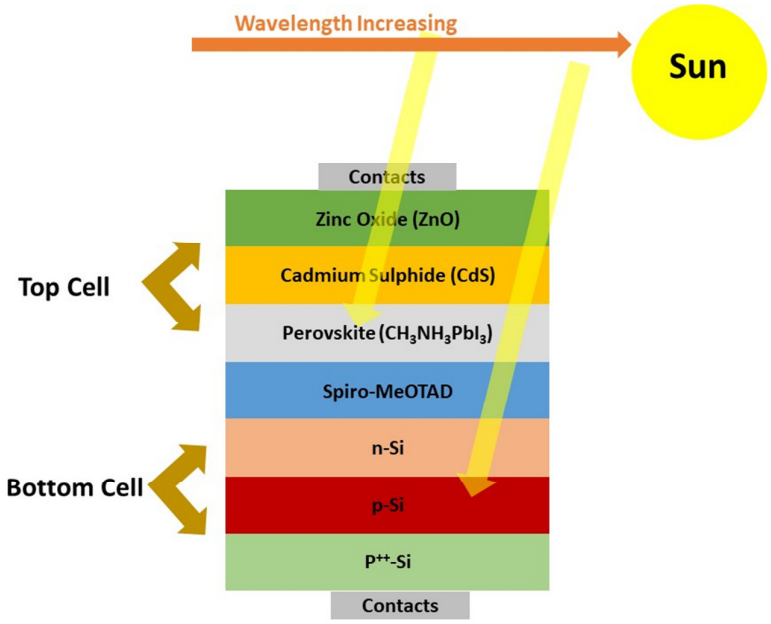

Figure 1: Schematic structure of the proposed tandem junction solar cell.

Table 1: Values of various parameters used in the present simulation.

Parameters	n-Zno [20]	n-CdS [21]	Perovskite [22]	Spiro-MeOTAD [24]	n-Si	P-Si [25]	P^{++}Si
Thickness, µm	0.01	0.02	0.5	0.02	0.02	80	0.1
Bandgap, Eg (eV)	3.37	2.44	1.5	3	1.1	1.1	1.1
Electron affinity, Xe (eV)	4.45	4.4	3.9	2.2	4.05	4.05	4.05
Dielectric constant, ε_r	9	10	6.5	3	11.9	11.9	11.9
Density of states in conduction band, NC (cm−3)	2.20E+18	2.20E+18	2.20E+18	2.20E+18	2.80E+19	2.80E+19	2.80E+19
Density of states in valence band, NV (cm−3)	1.80E+19	1.80E+19	1.80E+19	1.80E+19	2.60E+19	2.60E+19	2.60E+19
Mobility of electron µn (cm2/Vs)	100	100	2	2.00E-04	1.04E+03	1.04E+03	1.04E+03
Mobility of holes, µp (cm2/Vs)	25	25	2	2.00E-04	4.21E+02	4.21E+02	4.210 + 2
Donar concentration ND (cm−3)	1.00E+17	1.00E+18	-	-	1.00E+16	-	-
Acceptor concentration NA (cm−3)	-	-	1.00E+14	2.00E+16	-	1.00E+14	1.00E+22

The suggested model was created in SCAPS-1D, and AM 1.5 illumination was used for every simulation. Belgium's University of Gent created the one-dimensional program SCAPS. [26, 27, 28, 29, 30]. The software possesses the capability to accurately measure the following parameters: temperature, light bias, generation and recombination profile, illumination from both the p-side and n-side, capacitance-voltage and frequency spectroscopy, band structure of heterojunctions, short-current density, open-circuit voltage, quantum efficiency, and fill factor [30]. In earlier research, it has been widely used to

simulate different kinds of solar cells [31], [32], [33], [34], [35]. We focused on the electrical characteristics of tandem solar cells in our analysis, which includes the Poisson equations for electrons and holes as well as continuity.

3. Results and Discussion

The solar cell should be built to absorb as many incoming photons as possible in order to increase efficiency. We simulated a tandem cell by layering a perovskite material with a wide bandgap (1.5 eV) atop a silicon layer, with a tunnel/recombination layer in between to maximize solar photon absorption. Silicon, known for its ability for the absorption of photons of high-wavelength (such as those in the near-infrared region), is selected as the optimal material for the sub-cell at the bottom in tandem junction solar cells, while the sub-cell at the top absorbs low-wavelength photons (in the visible range).As a result, more photons are absorbed than would be possible with a single absorber layer, improving the solar cell's power conversion efficiency [36]. Moreover, the tandem technique will lessen silicon's thermalization losses caused by its narrow bandgap. In the sections that follow, we adjusted and refined a number of crucial cell parameters in order to increase the suggested structure's efficiency.

3.1 Effect of perovskite layer

As the proposed design revolves around a monolithic tandem solar cell, an inter-band tunnel connection is established to link the two absorber layers in series. Achieving an effective tandem device requires careful consideration of matching of current amid the top and bottom sub-cells and the incident photons transmission. This balance can be attained by the thickness adjustment and by regulating the bandgap of the sub-cell at the top [37]. Balancing Jsc in each sub-cell is crucial, as it is limited in tandem junction solar cells, connected in series, by the lowermost current of the sub-cell [38]. Initially, the perovskite sub-cell bandgap was altered from 1.3 to 1.7 eV to enhance efficiency, as this parameter highly influences the cell's photovoltaic performance [39]. As illustrated in Fig. 2, it is noticed that efficiency decreases as bandgap grows. It is also investigated how bandgap affects quantum efficiency (Q.E.), and as Fig. 3 illustrates, Q.E. seems to vary more at shorter wavelength ranges. Subsequently, the top sub-cell's thickness is adjusted between 0.1 and 1.0 μm. As demonstrated in Fig. 4, efficiency increases as thickness increases. The optimal thickness of 0.50μm is chosen for the top sub-cell in this case since it is noticed that after that, the rate of efficiency rise with perovskite layer thickness slows down. The significant efficiency

achieved with narrow thickness can be attributed to minimal losses due to recombination, like Shockley-Red-Hall (SRH) recombination, which usually arises in bulk devices [36]. These findings validate the substantial influence of the top sub-cell on the photovoltaic properties of the solar cell.

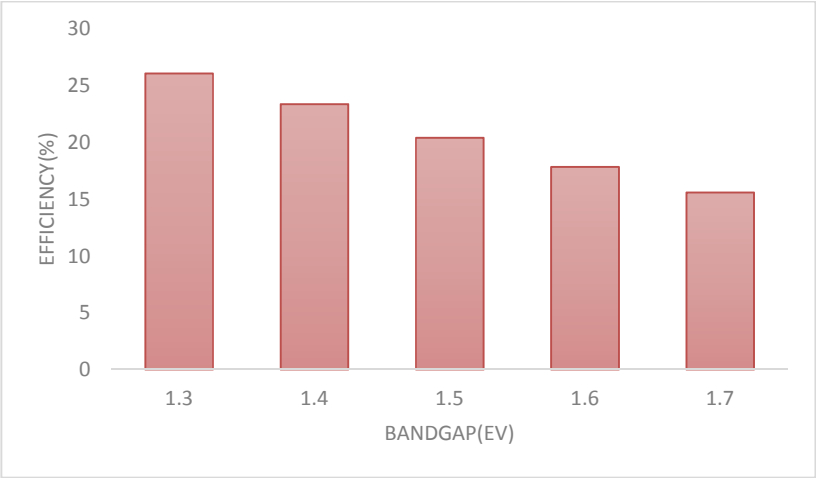

Figure 2: Variation of solar cell efficiency with bandgap of perovskite layer

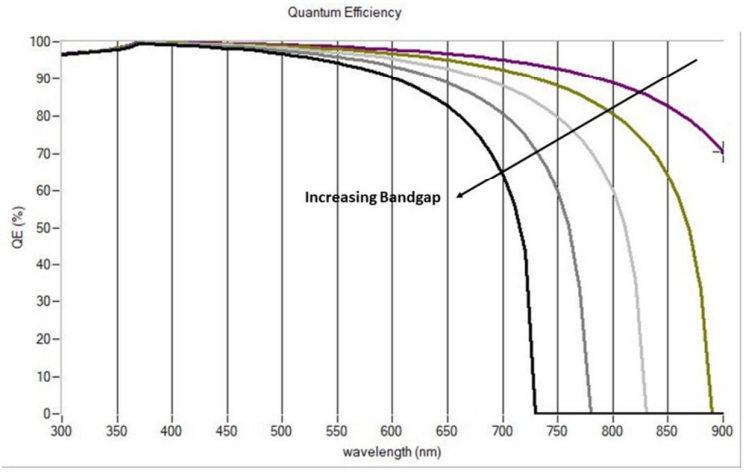

Figure 3: Influence of bandgap on the quantum efficiency v/s wavelength curve

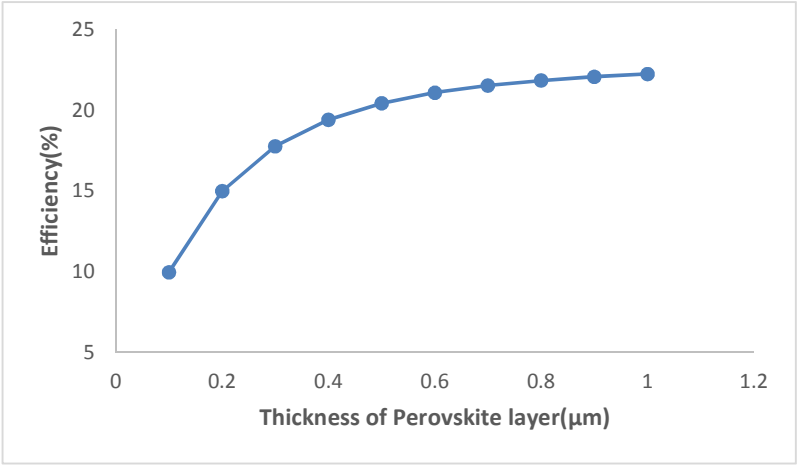

Figure 4: Effect of the thickness of perovskite layer on the solar cell efficiency

3.2 Effect of Shunt Resistance

It is not possible to immediately extrapolate from shunts' impact on single junction solar cells to multijunction solar cells. Just as shunted silicon solar cells within a module, shunt resistance effects in MJSCs can impact the V_{oc} and P_{max} voltage ranges while not affecting current generation [40]. The solar cell's efficiency was examined by adjusting the shunt resistance from 500 to 5000 Ohm cm^2, as depicted in Figure 5. It was noted that the solar cell's efficiency rose with increasing shunt resistance. Since the presence of shunts provides extra pathways for the current and lowers the coupling current, the influence of shunt resistance on coupling effects is substantial. The unintentional current leakage routes that avoid the photovoltaic junction and produce shunt currents decrease as the shunt resistance rises. More of the generated current passes through the designated photovoltaic channel when leakage currents are lower. Because there is less leakage, the effective current is higher, which improves performance.

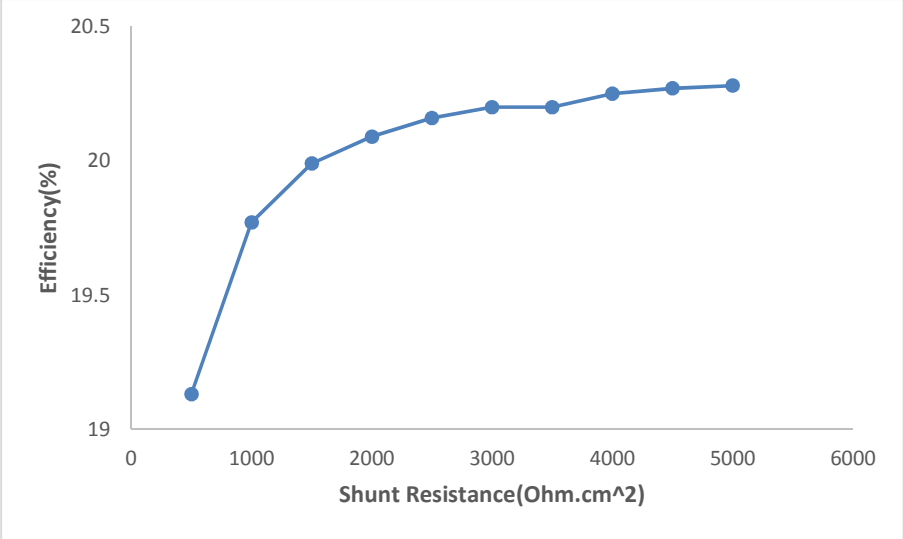

Figure 5: Variation in solar cell efficiency with shunt resistance

3.3 Effect of Series Resistance

As presented in Fig. 6, the series resistance of the multijunction solar cell was attuned from 1 to 10 Ohm cm^2 to assess its effect on efficiency. It is apparent that the efficiency of the solar cell declines noticeably with increasing series resistance. The semiconductor bandgap has a major role in determining the amplitude to which series resistance influences cell efficiency [41]. Low bandgap materials seem to have higher series resistance losses. Indeed, because low bandgap materials can absorb light over a wide range of wavelengths, larger

photocurrent is created in them at fixed illumination intensity. As a result, their electrical properties deteriorate more quickly than those of high bandgap materials. The cell design must prioritize minimizing series resistance, and by carefully adjusting the electrical gaps in the multijunction, the negative impact of series resistance losses can be significantly lessened.

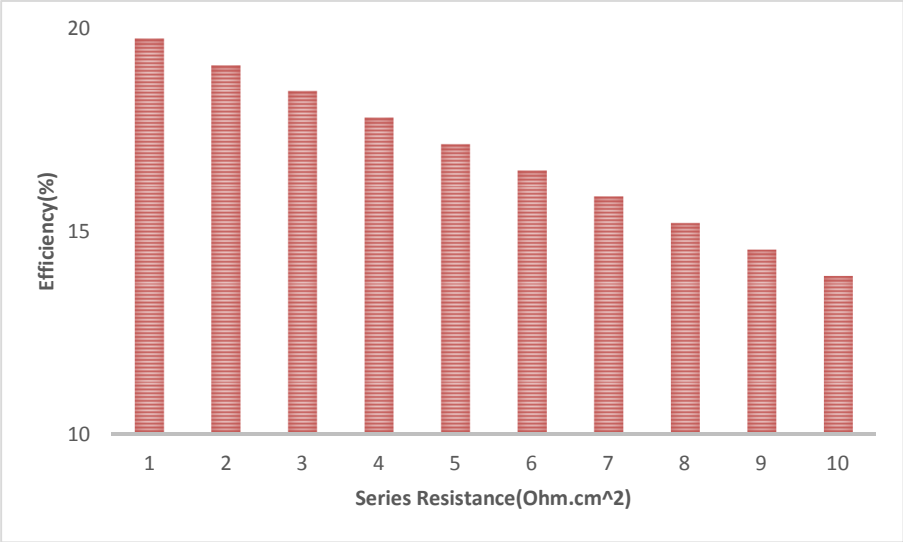

Figure 6: Variation in efficiency of the multijunction solar cell with series resistance.

4. Conclusion

One of the most encouraging technologies for achieving high efficiency solar to electricity conversion is multi-junction (MJ) solar cells. In the present work, we studied the potential efficiencies of a tandem solar cell made of perovskites and silicon under single-sun radiation. High efficiency solar cells are presented by the suggested model as a result of incoming photons' broadband absorption. By choosing the right perovskite layer bandgap, the multi-junction cell's performance is improved, and it is discovered that high efficiency is achieved with a perovskite material with an E_g = 1.5eV. Reducing the perovskite layer's thickness to 0.5µm improves the structure even further. Analysis was also done on the impact of series and shunt resistance on photovoltaic performance. These parasitic resistances must be identified and understood since they are essential for analyzing how PV modules function when working in real-world scenarios and for predicting probable failures.

Acknowledgements

Authors would like to thank Prof. Mark Burgleman and his co-workers, University of Ghent, Belgium for providing SCAPS-1D simulation software.

References

[1] S. De Wolf *et al.*, "Organometallic halide perovskites: sharp optical absorption edge and its relation to photovoltaic performance," *J Phys Chem Lett*, vol. 5, no. 6, pp. 1035–1039, 2014.

[2] S. D. Stranks *et al.*, "Electron-hole diffusion lengths exceeding 1 micrometer in an organometal trihalide perovskite absorber," *Science (1979)*, vol. 342, no. 6156, pp. 341–344, 2013.

[3] G. E. Eperon, S. D. Stranks, C. Menelaou, M. B. Johnston, L. M. Herz, and H. J. Snaith, "Formamidinium lead trihalide: a broadly tunable perovskite for efficient planar heterojunction solar cells," *Energy Environ Sci*, vol. 7, no. 3, pp. 982–988, 2014.

[4] K. Kacha, F. Djeffal, H. Ferhati, D. Arar, and M. Meguellati, "Numerical investigation of a double-junction a: SiGe thin-film solar cell including the multi-trench region," *Journal of Semiconductors*, vol. 36, no. 6, p. 064004, 2015.

[5] T. Todorov, T. Gershon, O. Gunawan, C. Sturdevant, and S. Guha, "Perovskite-kesterite monolithic tandem solar cells with high open-circuit voltage," *Appl Phys Lett*, vol. 105, no. 17, 2014.

[6] T. Todorov *et al.*, "Monolithic perovskite□CIGS tandem solar cells via in situ band gap engineering," *Adv Energy Mater*, vol. 5, no. 23, p. 1500799, 2015.

[7] N. N. Lal, Y. Dkhissi, W. Li, Q. Hou, Y. Cheng, and U. Bach, "Perovskite tandem solar cells," *Adv Energy Mater*, vol. 7, no. 18, p. 1602761, 2017.

[8] S. Albrecht *et al.*, "Towards optical optimization of planar monolithic perovskite/silicon-heterojunction tandem solar cells," *Journal of Optics*, vol. 18, no. 6, p. 064012, 2016.

[9] L. Kranz *et al.*, "High-efficiency polycrystalline thin film tandem solar cells," *J Phys Chem Lett*, vol. 6, no. 14, pp. 2676–2681, 2015.

[10] I. Almansouri, A. Ho-Baillie, and M. A. Green, "Ultimate efficiency limit of single-junction perovskite and dual-junction perovskite/silicon two-terminal devices," *Jpn J Appl Phys*, vol. 54, no. 8S1, p. 08KD04, 2015.

[11] F. T. Si *et al.*, "Quadruple-junction thin-film silicon-based solar cells with high open-circuit voltage," *Appl Phys Lett*, vol. 105, no. 6, 2014.

[12] F. Urbain, V. Smirnov, J.-P. Becker, A. Lambertz, U. Rau, and F. Finger, "Light-induced degradation of adapted quadruple junction thin film silicon solar cells for photoelectrochemical water splitting," *Solar Energy Materials and Solar Cells*, vol. 145, pp. 142–147, 2016.

[13] B. Liu *et al.*, "High efficiency and high open-circuit voltage quadruple-junction silicon thin film solar cells for future electronic applications," *Energy Environ Sci*, vol. 10, no. 5, pp. 1134–1141, 2017.

[14] S. Albrecht *et al.*, "Monolithic perovskite/silicon-heterojunction tandem solar cells processed at low temperature," *Energy Environ Sci*, vol. 9, no. 1, pp. 81–88, 2016.

[15] F. Sahli *et al.*, "Improved optics in monolithic perovskite/silicon tandem solar cells with a nanocrystalline silicon recombination junction," *Adv Energy Mater*, vol. 8, no. 6, p. 1701609, 2018.

[16] S. Essig *et al.*, "Raising the one-sun conversion efficiency of III–V/Si solar cells to 32.8% for two junctions and 35.9% for three junctions," *Nat Energy*, vol. 2, no. 9, pp. 1–9, 2017.

[17] J. Zheng *et al.*, "21.8% efficient monolithic perovskite/homo-junction-silicon tandem solar cell on 16 cm2," *ACS Energy Lett*, vol. 3, no. 9, pp. 2299–2300, 2018.

[18] H. Ferhati and F. Djeffal, "Exceeding 30% efficiency for an environment-friendly tandem solar cell based on earth-abundant Se/CZTS materials," *Physica E Low Dimens Syst Nanostruct*, vol. 109, pp. 52–58, 2019.

[19] E. Köhnen *et al.*, "Highly efficient monolithic perovskite silicon tandem solar cells: analyzing the influence of current mismatch on device performance," *Sustain Energy Fuels*, vol. 3, no. 8, pp. 1995–2005, 2019.

[20] K. Ueda, H. Tabata, and T. Kawai, "Magnetic and electric properties of transition-metal-doped ZnO films," *Appl Phys Lett*, vol. 79, no. 7, pp. 988–990, 2001.

[21] L. Ma, X. Ai, and X. Wu, "Effect of substrate and Zn doping on the structural, optical and electrical properties of CdS thin films prepared by CBD method," *J Alloys Compd*, vol. 691, pp. 399–406, 2017.

[22] M. Hirasawa, T. Ishihara, T. Goto, K. Uchida, and N. Miura, "Magnetoabsorption of the lowest exciton in perovskite-type compound (CH3NH3) PbI3," *Physica B Condens Matter*, vol. 201, pp. 427–430, 1994.

[23] J. F. Klem and J. C. Zolper, "Semiconductor tunnel junction with enhancement layer," Sandia National Laboratories (SNL), Albuquerque, NM, and Livermore, CA …, 1997.

[24] L. Huang *et al.*, "Electron transport layer-free planar perovskite solar cells: further performance enhancement perspective from device simulation," *Solar Energy Materials and Solar Cells*, vol. 157, pp. 1038–1047, 2016.

[25] M. S. Shur, *Handbook series on semiconductor parameters*, vol. 1. World Scientific, 1996.

[26] J. Verschraegen and M. Burgelman, "Numerical modeling of intra-band tunneling for heterojunction solar cells in SCAPS," *Thin Solid Films*, vol. 515, no. 15, pp. 6276–6279, 2007.

[27] K. Decock, S. Khelifi, and M. Burgelman, "Modelling multivalent defects in thin film solar cells," *Thin Solid Films*, vol. 519, no. 21, pp. 7481–7484, 2011.

[28] M. Burgelman, P. Nollet, and S. Degrave, "Modelling polycrystalline semiconductor solar cells," *Thin Solid Films*, vol. 361, pp. 527–532, 2000.

[29] M. Burgelman, J. Verschraegen, S. Degrave, and P. Nollet, "Modeling thin□film PV devices," *Progress in Photovoltaics: Research and Applications*, vol. 12, no. 2□3, pp. 143–153, 2004.

[30] A. Shalav, B. S. Richards, T. Trupke, K. W. Krämer, and H.-U. Güdel, "Application of NaYF4: Er3+ up-converting phosphors for enhanced near-infrared silicon solar cell response," *Appl Phys Lett*, vol. 86, no. 1, 2005.

[31] A. S. Mathur, S. Dubey, Nidhi, and B. P. Singh, "Study of role of different defects on the performance of CZTSe solar cells using SCAPS," *Optik (Stuttg)*, vol. 206, p. 163245, 2020, doi: https://doi.org/10.1016/j.ijleo.2019.163245.

[32] S. Dubey, A. S. Mathur, Nidhi, and B. P. Singh, "Effect of defect density in different layers and ambient temperature of n-i-p a-Si single junction solar cells performance," *International Journal of Scientific Research in Physics and Applied Sciences*, vol. 7, no. 2, pp. 93–98, 2019, [Online]. Available: http://inis.iaea.org/search/search.aspx?orig_q=RN:50046103

[33] B. Sharma, A. S. Mathur, I. K. Singh, and B. P. Singh, "Performance optimization of non-fullerene acceptor organic solar cell by incorporating carbon nanotubes as

flexible transparent electrode," *Results in Optics*, vol. 9, p. 100315, 2022, doi: https://doi.org/10.1016/j.rio.2022.100315.

[34] B. Sharma, A. S. Mathur, V. K. Rajput, I. K. Singh, and B. P. Singh, "Device modeling of non-fullerene organic solar cell by incorporating CuSCN as a hole transport layer using SCAPS," *Optik (Stuttg)*, vol. 251, p. 168457, 2022, doi: https://doi.org/10.1016/j.ijleo.2021.168457.

[35] A. S. Mathur *et al.*, "Role of absorber and buffer layer thickness on Cu2O/TiO2 heterojunction solar cells," *Solar Energy*, vol. 233, pp. 287–291, 2022, doi: https://doi.org/10.1016/j.solener.2022.01.047.

[36] M. A. Green, "Solar cells: operating principles, technology, and system applications," *Englewood Cliffs*, 1982.

[37] Q. Wali, N. K. Elumalai, Y. Iqbal, A. Uddin, and R. Jose, "Tandem perovskite solar cells," *Renewable and Sustainable Energy Reviews*, vol. 84, pp. 89–110, 2018.

[38] R. R. King *et al.*, "40% efficient metamorphic GaInP⁄GaInAs⁄Ge multijunction solar cells," *Appl Phys Lett*, vol. 90, no. 18, 2007.

[39] M. T. Hörantner *et al.*, "The Potential of Multijunction Perovskite Solar Cells," *ACS Energy Lett*, vol. 2, no. 10, pp. 2506–2513, Oct. 2017, doi: 10.1021/acsenergylett.7b00647.

[40] J. Wohlgemuth and W. Herrmann, "Hot spot tests for crystalline silicon modules," in *Conference Record of the Thirty-first IEEE Photovoltaic Specialists Conference, 2005.*, 2005, pp. 1062–1063. doi: 10.1109/PVSC.2005.1488317.

[41] A. Vossier, F. Gualdi, A. Dollet, R. Ares, and V. Aimez, "Approaching the Shockley-Queisser limit: General assessment of the main limiting mechanisms in photovoltaic cells," *J Appl Phys*, vol. 117, no. 1, p. 015102, Jan. 2015, doi: 10.1063/1.4905277.

Cite this Article:

Prem Pratap Singh and Kripa Shanker Singh, " ***Simulation study of Perovskite/Si Monolithic Multijunction Solar Cell*** *", International Journal of Scientific Research in Modern Science and Technology (IJSRMST), ISSN: 2583-7605 (Online), Volume 3, Issue 1, pp. 41-52, January 2024.*

Journal URL: ***https://ijsrmst.com/***

DOI: ***https://doi.org/10.59828/ijsrmst.v3i1.177***